

A ‘constant Lagrangian’ model for galactic dynamics in a geodetic approach towards the galactic rotation Dark Matter issue.

E.P.J. de Haas^{1, a)}

Nijmegen, The Netherlands

(Dated: April 22, 2018)

I start with a historical note on the galactic rotation curves issue. The problem with the virial theorem in observed galactic dynamics, lead to the Dark Matter hypothesis but also to Modified Newtonian Dynamics or MOND. Then I move (away) from MOND towards a relativistic, Lagrangian approach of orbital dynamics in a curved Schwarzschild metric. I propose a ‘constant Lagrangian’ model for galactic scale geodetic dynamics. I will show with four rotation fitting curves to what extend my proposed model galaxies ‘constant Lagrangian’ postulate works in these limited number of situations. The fitted galaxies are NGC 2403, NGC 3198, UGC 6614 and F571-8. In the paper I present a theoretical context in which the ‘constant Lagrangian’ postulate might replace the classical virial theorem on a galactic scale. But the proposed postulate isn’t a ‘general law of nature’ because in the solar system and in the GNSS relativistic context, the classical virial theorem is proven accurate. Due to the limitations of the proposed postulate, a statement regarding Dark Matter can’t be made. But the model might achieve within the GR-Schwarzschild paradigm what MOND achieves within the Newtonian paradigm, fitting the experimental galactic rotation curves.

PACS numbers: 95.30.Sf, 95.35.+d

Keywords: Dark Matter, MOND, Schwarzschild, Galactic rotation curves

^{a)}Electronic mail: haas2u@gmail.com

CONTENTS

I. The virial theorem in trouble on the galactic scale.	3
II. MOND	4
III. Classical Lagrangian dynamics	6
IV. A geodetic approach of gravitational orbits	7
V. A relativistic virial theorem for a model galaxy	9
VI. Fitting four real galactic rotation curves	13
VII. Dark Matter, an unresolved issue	19
References	21

I. THE VIRIAL THEOREM IN TROUBLE ON THE GALACTIC SCALE.

In 1932 the Dutch astronomer Oort observed that the stars in the galactic vicinity of the Sun are moving peculiarly fast, almost 8 times as fast as could be inferred from the calculated Newtonian acceleration. Oort assumed that dark matter would be the cause of this apparent difference, with ‘dark’ referring to ordinary matter not seen by us due to various reasons (Oort, 1932).

In 1933 Dark Matter was mentioned as “dunkle Materie” in a paper by Zwicky. Fritz Zwicky was studying the Coma Cluster of galaxies and found that his calculations for orbital acceleration and stellar mass within it was off by a large factor. He concluded that there should be a much greater density of dark matter within the cluster than there was luminous matter. Zwicky concluded that this constituted an unsolved problem (Zwicky, 1933). In 1937 Zwicky regarded his study on the Coma Cluster a test of Newton’s law of gravity on the largest cosmological scale possible, by applying the virial theorem on a cluster of galaxies. He also mentioned in his 1937 paper the possibility to test the virial theorem by applying it to the rotational velocities of the individual stars in the separate galaxies. But he concluded that this was technologically out of reach (Zwicky, 1937).

The breakthrough research of Rubin and Ford around 1970-1975 established beyond doubt the outer rotational velocity curves of individual galaxies, which turned out to be flat (Rubin et al., 1978). This was in conflict with velocity curves that resulted from the application of the virial theorem to the luminous mass of these galaxies. Rubin and Ford cited colleagues who suggested the existence of a large galactic halo of dark matter. In a 1980 paper presenting further research they concluded that the form of the rotation curves implied that significant non-luminous mass should be located at large distances beyond the optical galaxy. The total mass of a galaxy should, for large distances, increase at least as fast as the distance from the center (Rubin et al., 1980).

The third major evidence for Dark Matter was the gravitational lensing effect of clusters of galaxies. The mass of stars and hot gas in clusters who collectively act as a gravitational lens is too small to bend the light from the background galaxies as much as they actually do. A large density of dark matter in the center of these cluster is needed to explain the strength of the observed lensing effect (Koopmans et al., 2009).

In the course of decades it has become more and more clear that ordinary matter can’t

be the cause of those observed phenomena. That realization caused the term ‘dark matter’ to evolve into ‘Dark Matter’, with the capital letters indicating its elusive character. Today it has been predominantly, but not unanimously, been accepted that non-baryonic particles must exist in the calculated densities. A range of different astrophysical measurements point in this direction. I quote:

Astrophysical observations have provided compelling evidence for the existence of a non-baryonic dark component of the universe: dark matter (DM). The currently most accurate, although somewhat indirect, determination of DM abundance comes from global fits of cosmological parameters to a variety of observations, while the nature of DM remains largely unknown. One of the candidates for a DM particle is a weakly interacting massive particle (WIMP). (The ATLAS Collaboration, 2018)

II. MOND

One of the few non-particle approaches to the problem of Dark Matter is MOND or MOdified Newtonian Dynamics. MOND started in 1983 with two seminal paper of Milgrom. I quote from his papers:

All determinations of dynamical mass within galaxies and galaxy systems make use of a virial relation of the form $V^2 = MGr^{-1}$ where V is some typical velocity of particles in the system, r is of the order of the size of the system, M is the mass to be determined, and G is the gravitational constant. [...] It must have occurred to many that there may, in fact, not be much hidden mass in the universe and that the dynamical masses determined on the basis of the above virial relation are gross overestimates of the true gravitational masses. (Milgrom, 1983b)

I have considered the possibility that Newton’s second law does not describe the motion of objects under the conditions which prevail in galaxies and systems of galaxies. In particular I allowed for the inertia term not to be proportional to the acceleration of the object but rather be a more general function of it. With some simplifying assumptions I was led to the form

$$m_g \mu \left(\frac{a}{a_0} \right) \mathbf{a} = \mathbf{F},$$

replacing $m_g \mathbf{a} = \mathbf{F}$. [...] For accelerations much larger than the acceleration constant (a_0), $\mu \approx 1$, and the Newtonian dynamics is restored. (Milgrom, 1983b)

I use a modified form of the Newtonian dynamics (inertia and/or gravity) to describe the motion of bodies in the gravitational fields of galaxies, assuming that galaxies contain no hidden mass, with the following main results. 1. The Keplerian, circular velocity around a finite galaxy becomes independent of r at large radii, thus resulting in asymptotically flat velocity curves. 2. The asymptotic circular velocity (V_∞) is determined only by the total mass of the galaxy (M): $V_\infty^4 = a_0 GM$, where a_0 is an acceleration constant appearing in the modified dynamics. This relation is consistent with the observed Tully-Fisher relation if one uses a luminosity parameter which is proportional to the observable mass. (Milgrom, 1983a)

The original Tully-Fisher relation is a relation between the luminosity of a spiral galaxy and its, maximum, rotation velocity (Tully and Fisher, 1977). The physical basis of the Tully-Fisher relation is the relation between a galaxy's total baryonic mass and the velocity at the flat end of the rotation curve, the final velocity. According to McGaugh both stellar and gas mass of galaxies have to be taken into account in the relation that is referred to as the Baryonic Tully-Fisher (BTF) relation (McGaugh, 2005). In 2005 McGaugh determined the baryonic version of the LT relation as $M_d = 50v_f^4$, see (McGaugh, 2005) and Fig(1). In this form, M_d is expressed in solar mass $M_\odot = 1,99 \cdot 10^{30} \text{ kg}$ units and the final velocity of the galactic rotation velocity curve v_f is expressed in km/s . If we express the galactic mass in kg and the velocity in m/s we get the total baryonic mass, final velocity relations in SI unit values as $M_b = 1,0 \cdot 10^{20} v_f^4$.

In 1983, Milgrom interpreted the BTF relation as an indication of a deviation from Newtonian gravity, making a modification of Newtonian dynamics or MOND necessary (Milgrom, 1983b). Using McGaug's 2005 values in SI units, Milgrom presented the BTF relation in the form $v_f^4 = 1,0 \cdot 10^{-20} M_b = Ga_0 M_b$, resulting in an acceleration $a_0 = 1,5 \cdot 10^{-10} \text{ m/s}^2$ in McGaug's values. Milgrom hypothesized that this relation should hold exactly, thus interpreting it as an inductive law of nature instead of looking at it as just an empirical relation (Milgrom, 1983a). The resulting acceleration can be written as $5 \cdot a_0 \approx cH_0$, with the velocity of light c and the Hubble constant H_0 . According to Milgrom, the deeper significance

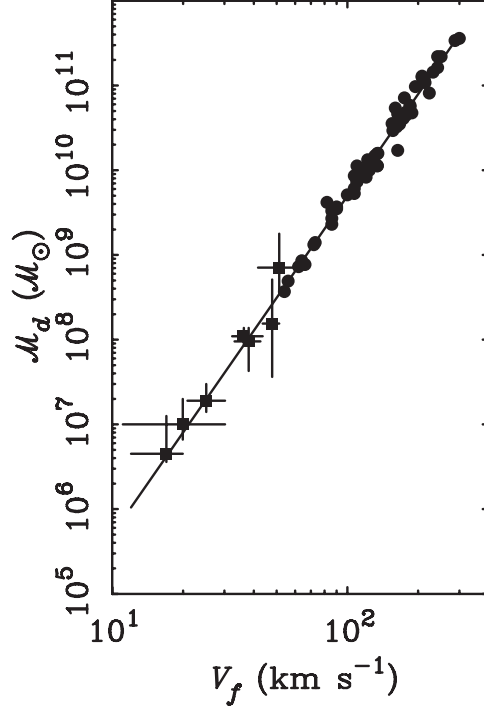


FIG. 1. The Baryonic Tully-Fisher relation. Reprint from McGaugh 2005 (McGaugh, 2005).

of this relation between this special galactic acceleration and the Hubble acceleration should be revealed by future cosmological insights (Milgrom, 1983b).

III. CLASSICAL LAGRANGIAN DYNAMICS

The Lagrangian equation of motion reads

$$\frac{d}{dt} \left(\frac{\partial L}{\partial \dot{q}} \right) - \frac{\partial L}{\partial q} = 0. \quad (1)$$

In classical gravitational dynamics I assume circular orbits with $\dot{q} = v$ and $q = r$. The Lagrangian itself is then given by $L = K - V$, with V the Newtonian potential gravitational energy and K the kinetic energy. One then gets

$$\frac{d}{dt} \left(\frac{\partial L}{\partial \dot{q}} \right) = \frac{dp}{dt} = F. \quad (2)$$

The other part gives

$$\frac{\partial L}{\partial q} = -\frac{dV}{dr}, \quad (3)$$

so one gets Newton's equation of motion in a central field of gravity

$$F_g = -\frac{dV}{dr}. \quad (4)$$

Further analysis of the context results in the identification of the Hamiltonian of the system, $H = K + V$, as being a constant of the orbital motion and the virial theorem as describing a relation between K and V in one single orbit but also between different orbits, $2K + V = 0$.

On the galactic scale it is assumed that velocities are so low and gravitational fields are so weak, that Newtonian mechanics suffices and not much of relativity is needed. The problem with the rotational velocities of stars in galaxies and galaxies in cluster of galaxies is thus supposed to be a Newtonian physics issue that can be dealt with in the dynamics described above. The Dark Matter solution to the too fast rotational galactic velocities has two faces. On the one hand one tries to describe the density distribution of Dark Matter, needed in order to match the measurements with classical dynamics, specifically the virial theorem. On the other hand one tries to identify the Dark Matter constituents, usually seen as an out-of-the-box extension of the known Standard Model of particle physics.

IV. A GEODETIC APPROACH OF GRAVITATIONAL ORBITS

The problem with the previous analysis is connected to the notion of geodesic motion in General Relativity. The problem can best be described in a semi-relativistic approach using the classical Lagrangian equation of motion for geodesic orbits. The most important aspect of geodesic motion in GR is that it requires no force to move on a geodesic. This has important implications for the Lagrangian equation of motion, because $F = 0$ on a geodesic. One gets

$$\frac{d}{dt} \left(\frac{\partial L}{\partial \dot{q}} \right) = F_g = 0 \quad (5)$$

and as a consequence also

$$\frac{\partial L}{\partial q} = -\frac{dL}{dr} = 0. \quad (6)$$

As a result, one gets the crucial

$$L = K - V = \text{constant} \quad (7)$$

on geodesic orbits.

This result, the Lagrangian of the system as being the constant of the geodesic motion, is used on a daily basis by many of us because it is used by GNSS systems for the relativistic correction of atomic clocks in their satellites. Let's elaborate this a bit further. In General

Relativity, the proper time-rate $d\tau$ is defined through the metric distance ds as $ds \equiv cd\tau$. The square metric distance is defined through

$$ds^2 \equiv g_{\mu\nu}dx^\mu dx^\nu. \quad (8)$$

Given coordinate world time-rate dt , which is the time-rate of a standard clock at a position where $d\tau = dt$ (in GR-Schwarzschild this implies a clock at rest at infinity), we get the general

$$\frac{ds^2}{dt^2} = \frac{c^2 d\tau^2}{dt^2} = g_{\mu\nu} \frac{dx^\mu}{dt} \frac{dx^\nu}{dt} = g_{\mu\nu} V^\mu V^\nu, \quad (9)$$

with the geodesic four-vector velocity V^μ . In this equation, $d\tau$ stands for the local proper clock-rate of a clock in a geodetic orbit in a field of gravity and dt is the universal clock-rate. Because of this interpretation of dt , the velocity V^μ is the velocity as seen from a position where $d\tau = dt$. See for example (Singer, 1956), (Weinberg, 1972, p. 79), (Misner et al., 1973, p. 1054-1055), (Straumann, 1984, p. 97), (Ohanian and Ruffini, 2013, p. 119).

In case of the Schwarzschild metric in polar coordinates, we have (Ruggiero et al., 2008)

$$ds^2 = \left(1 + \frac{2\Phi}{c^2}\right) c^2 dt^2 - \left(1 + \frac{2\Phi}{c^2}\right)^{-1} dr^2 - r^2 d\theta^2 - r^2 \sin^2\theta d\phi^2. \quad (10)$$

In case of a clock on a circular geodesic on the equator of a central non-rotating mass M we have $\frac{dr}{dt} = 0$, $\frac{d\theta}{dt} = 0$, $\sin\theta = 1$ and $\frac{d\phi}{dt} = \omega$. We thus get

$$\frac{ds^2}{dt^2} = \frac{c^2 d\tau^2}{dt^2} = \left(1 + \frac{2\Phi}{c^2}\right) c^2 - r^2 \omega^2 \quad (11)$$

and

$$\frac{d\tau^2}{dt^2} = 1 + \frac{2\Phi}{c^2} - \frac{r^2 \omega^2}{c^2}. \quad (12)$$

With $v_{orbit} = r\omega$ we have

$$\frac{d\tau^2}{dt^2} = 1 + \frac{2\Phi}{c^2} - \frac{v_{orbit}^2}{c^2}. \quad (13)$$

So finally we get the GR result

$$\frac{d\tau}{dt} = \sqrt{1 + \frac{2\Phi}{c^2} - \frac{v_{orbit}^2}{c^2}} \quad (14)$$

with $d\tau$ as the clock-rate of a standard clock A in a geodetic orbit and dt as the ‘universal’ clock-rate G of a standard clock at rest in infinity, the only condition for which $d\tau = dt$. The result of Eqn. (14) is the basic relativistic correction used in GNSS clock frequencies, with the first as the gravity effect or gravitational potential correction and the second as the

velocity effect or the correction due to Special Relativity (Ashby, 2002; Hećimović, 2013; Delva and Lodewyck, 2013).

Given the classical definitions of $K = \frac{mv_{orbit}^2}{2}$ and $V = m\Phi$, we get

$$\frac{d\tau}{dt} = \sqrt{1 - \frac{2L}{U_0}}. \quad (15)$$

All the satellites of a GNSS system are being installed on a similar orbit and thus syntonized relative to one another because they share the same high and velocity and have constant L and $\frac{d\tau}{dt}$ on those orbits. But different GNSS systems, as for example GPS compared to GALILEO, are functioning on different orbits with different velocities and those systems aren't syntonized relative to one another. This non-syntonization between satellites on orbits with different heights and virial theorem connected velocities is very annoying for the effort towards realizing an integration of the different GNSS systems into one single global network.

V. A RELATIVISTIC VIRIAL THEOREM FOR A MODEL GALAXY

When I connected

$$\frac{d\tau^2}{dt^2} = 1 + \frac{2\Phi}{c^2} - \frac{v_{orbit}^2}{c^2} = 1 - \frac{2L}{U_0} \quad (16)$$

to the problem of the galactic rotation curve, I realized that the flat rotation curve implies atomic clock syntonization in those areas. In those outer regions, the potential can be assumed to be zero and the velocity constant. Those flat rotation rate zones are the GNSS engineer's dream come true. This made me curious as to the clock-rate status in the inner regions. The intriguing thing is that you can jump from orbit to orbit and still encounter a constant clock-rate on all the orbiting satellites you encounter on an imaginary voyage through the outer regions of galaxies. This implies that precisely in those regions where the classical virial theorem seems in trouble, $L \simeq constant$, not just in one single orbit *but also between different orbits*. It should be clear that for those geodetic orbits the classical virial theorem, which in its most essential form states that $F_{gravity} = F_{centripetal}$, becomes meaningless because on circular geodetics this reduces to the empty expression $0 = 0$.

In order to study the relativistic clock-rate behavior in the inner regions of galaxies, I had to construct a model galaxy. Real galaxies are way to fussy, complex and messed up to get interpretable results. My model galaxy is build of a model bulge with mass M and

radius R and a Schwarzschild metric emptiness around it. The model bulge has constant density $\rho_0 = \frac{M}{V} = \frac{3M}{4\pi R^3}$ and its composing stars rotate on geodetics in a quasi-solid way. So all those stars in the bulge have equal angular velocity on their geodetic orbits, with $v = \omega r$. On the boundary between the quasi solid spherical bulge and the emptiness outside of it, the orbital velocities are behaving smoothly. So the last star in the bulge and the first star in the Schwarzschild region have equal velocities and potentials. I also assume that the Newtonian potential itself is unchanged and unchallenged, remains classical in the whole galaxy and its surroundings. Such a model galaxy doesn't have a SMBH in the center of its bulge and it only has some very lonely stars in the space outside the bulge.

Point	Relation	Expression
Outside the bulge	$r > R$	$-\frac{GM}{r}$
On the Surface	$r = R$	$-\frac{GM}{R}$
Inside the bulge	$r < R$	$-GM \left[\frac{3R^2 - r^2}{2R^3} \right]$
At the centre	$r = 0$	$-\frac{3}{2} \left(\frac{GM}{R} \right)$

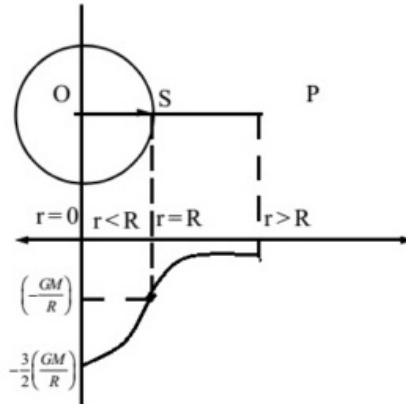


FIG. 2. The potential inside and out of a model bulge

The gravitational potential in such a case is well known, see Fig.(2). If this sphere would be in a condition where the classical virial theorem would hold, so $2K = -V$, then on the boundary $r = R$ we would have $K = \frac{GM}{2R}$ and $L = K - V = \frac{3GM}{2R}$. At the center of the rotating sphere, $K = 0$ and we also have $L = \frac{3GM}{2R}$.

From $r = 0$ to $r = R$, the potential Φ increased as r^2 . The kinetic energy does the same

because $v^2 = \omega^2 r^2$. One can conclude that they increase identically and that $L = K - V$ is a constant inside the quasi-solid sphere. We can write for the region from $r = 0$ to $r = R$

$$\frac{L}{m} = \frac{v_{orbit}^2}{2} + \frac{GM}{r} = \frac{3GM}{2R} = constant. \quad (17)$$

As a result, in such a model bulge, L is a constant of the motion, not only in one orbit but also between orbits. All the clocks in such a model bulge would be synchronized.

Thus, in the model galaxy that I am about to construct, we have $L = constant$ inside the model bulge and we have $L = constant$ in the outer regions where the rotational velocity curve flattens and the Newtonian potential turns negligibly small. So let's be bold and declare $L = K - V = constant$ in the entire galaxy, without changing the Newtonian potential. What would that have as effects?

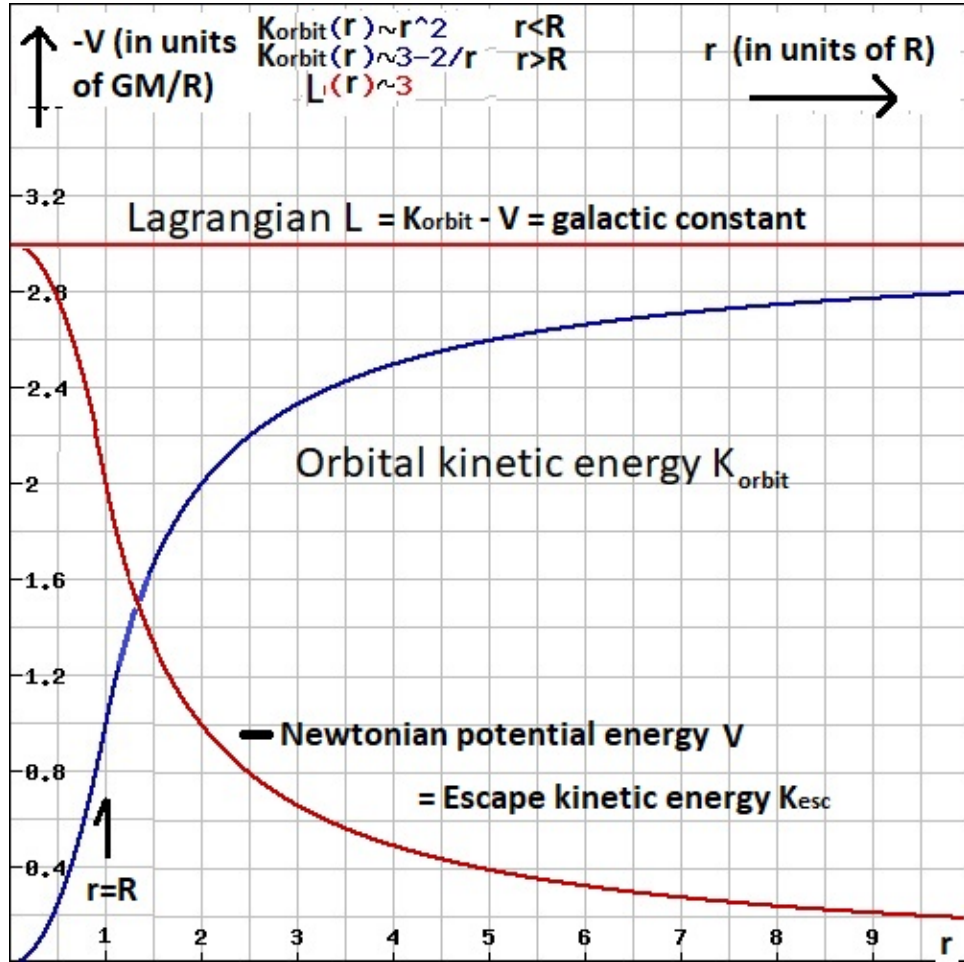


FIG. 3. The square of the orbital velocity profile in the model galaxy with $L = constant$.

We would get $K = L + V$ and $L = V(r = 0)$ so for the region $0 \leq r \leq R$ we get

$$v_{orbit}^2 = \frac{GM}{R} \cdot \frac{r}{R} \quad (18)$$

and outside the model bulge, where $R \leq r \leq \infty$, we have

$$v_{orbit}^2 = \frac{3GM}{R} - \frac{GM}{r}. \quad (19)$$

In Fig.(3) I sketched the result, with $-V = +K_{escape}$.

From the perspective of a free fall Einstein elevator observer, the free fall on a radial geodetic from infinity towards the center of the bulge, the other free fall tangential geodetics seem to abide the law of conservation of energy, because the escape kinetic energy plus the orbital kinetic energy is a constant on my model galaxy with galactic constant L . An Einstein elevator system with test mass m that would be put in an orbital collapse situation, magically descending from orbit to orbit in a process in thermodynamic equilibrium, would have constant total kinetic energy, from the radial free fall perspective. This can be expressed as $L = K_{orbit} - V = K_{orbit} + K_{escape} = K_{final}$.

Such a model galaxy would also be a GNSS engineer's dream come true because the whole model galaxy is in one single syntonized time-bubble.

$$\frac{d\tau}{dt} = \sqrt{1 - \frac{2L}{U_0}}. \quad (20)$$

Given the Baryonic Tully-Fisher relation in Milgrom's version $v_{final}^4 = Ga_0M$ with $2\pi a_0 \approx cH_0$, with a_0 as Milgrom's galactic minimum acceleration and H_0 as the Hubble constant, we get as a galactic time bubble fix

$$\frac{d\tau}{dt} = \sqrt{1 - \frac{2L}{U_0}} = \sqrt{1 - \frac{v_{final}^2}{c^2}} = \sqrt{1 - \sqrt{\frac{v_{final}^4}{c^4}}} = \quad (21)$$

$$\sqrt{1 - \sqrt{\frac{Ga_0M}{c^4}}} = \sqrt{1 - \sqrt{\frac{GH_0M}{2\pi c^3}}} = \sqrt{1 - \sqrt{\frac{M}{2\pi M_U}}}, \quad (22)$$

in which I used $L = 3GM/R = K_{final} = \frac{1}{2}mv_{final}^2$ and $M_U = \frac{c^3}{GH_0}$. This last constant can be referred to as an apparent mass of the Universe, a purely theoretical number constant, see (Mercier, 2015). In a model Universe, this would imply that my model galaxy would be in a proper time bubble with clock-rate $d\tau$ relative to the universal clock-rate dt in proportion to the masses of galaxy M and Universe M_U . In my model galaxy theoretical environment

the Baryonic Tully-Fisher relationship implies that the galactic time bubble is fixed through the mass of my model galaxy and that this fix is a cosmological one. So what is a universal acceleration minimum a_0 in MOND can be interpreted as a universally correlated (through M_U) but still local (through M) time bubble fix in my model galaxy geodetic environment.

This doesn't imply that I can integrate my model galaxy approach into MOND, because you either take the perspective of geodetic motion without any force of gravity, or you don't have a curved metric and use the classical gravitational acceleration approach. My approach of $L = \text{constant}$ started with setting $F_g = 0$ in the Lagrangian equation of motion. Milgrom started by modifying Newton's second law, leading to an adapted $F_g \neq 0$. You can't have it both ways. My approach of $L = \text{constant}$ and Milgrom's $F_g = ma\mu$ are mutually exclusive.

VI. FITTING FOUR REAL GALACTIC ROTATION CURVES

Having determined the model galactic velocity rotation curve based on the Lagrangian as a galactic constant of orbital motion, the question is to what extent real galaxies can be modeled in this way. For this I used the experimental velocity rotation data of four galaxies: NGC 2403, NGC 3198, UGC 6614 and F571-8. I plotted them in Excell. The velocity rotation curve data come from different sources. The NGC 2403 data are from (Begeman, 2006, p. 51). The UGC 6614 and F571-8 data are from (McGaugh et al., 2001) and were retrieved from the [data website of McGaugh](#). The NGC 3198 data are from (Karukes et al., 2015, p. 2) and brought to my attention by (Vossos and Vossos, 2017).

In this section I present the plots of V_{orb}^2 against r , with in each plot the experimental values in red stars and the theoretical values in black bars. The fitting plots are given in two versions. The first plot is with one single fit for M and R , this is the pure model. In the second plot the two parameters M and R are used as one single 'free' parameter for every single measurement, because the time-bubble or L is constant constraint leaves only one degree of freedom. The locked in through L variation of M and R in plot 2 can be monitored using the apparent model mass density of the bulge ρ_{bulge} . This density varies as M , with locked in R , varies. With this parameter freedom of one single value, M and with locked R in L and ρ_{bulge} , all four experimental curves could be fitted really nice. The most important cut in the model is the change from the model bulge to the model empty space around it. In the model bulge, $V_{orb}^2 \propto r^2$, outside the model bulge $V_{orb}^2 \propto -r^{-1}$. In the

fixed fitting curve, the apparent mass density of the bulge is the main variable that changes due to more realistic circumstances. The excell data sheets of the plots are in the appendix. The fact that it is possible to exactly plot the rotation curves with just one free parameter should be significant for the underlying physics. In my approach, one free parameter can force a time-bubble on a whole galaxy.

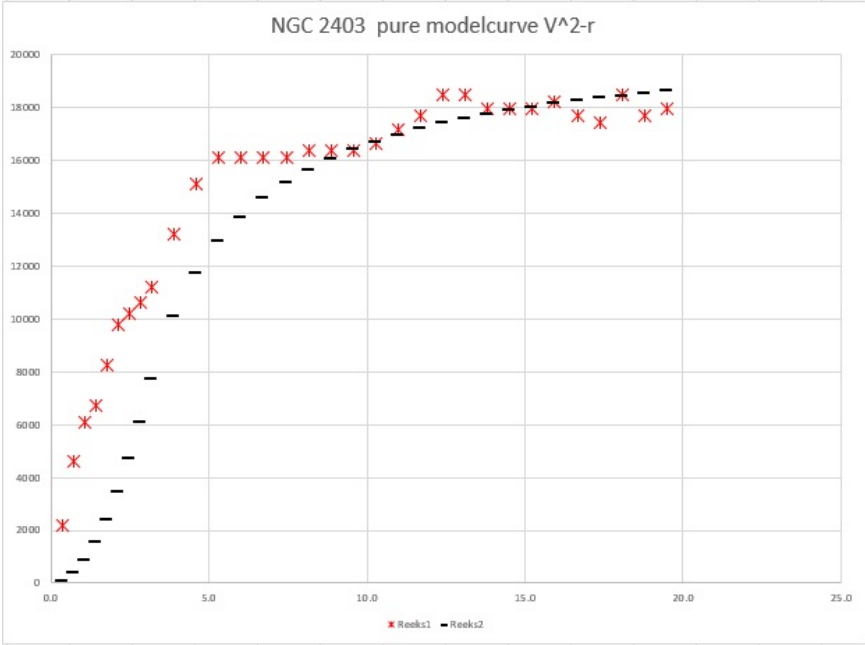


FIG. 4. UGC 2403 Plot1, V_{orb}^2 against r , pure model.

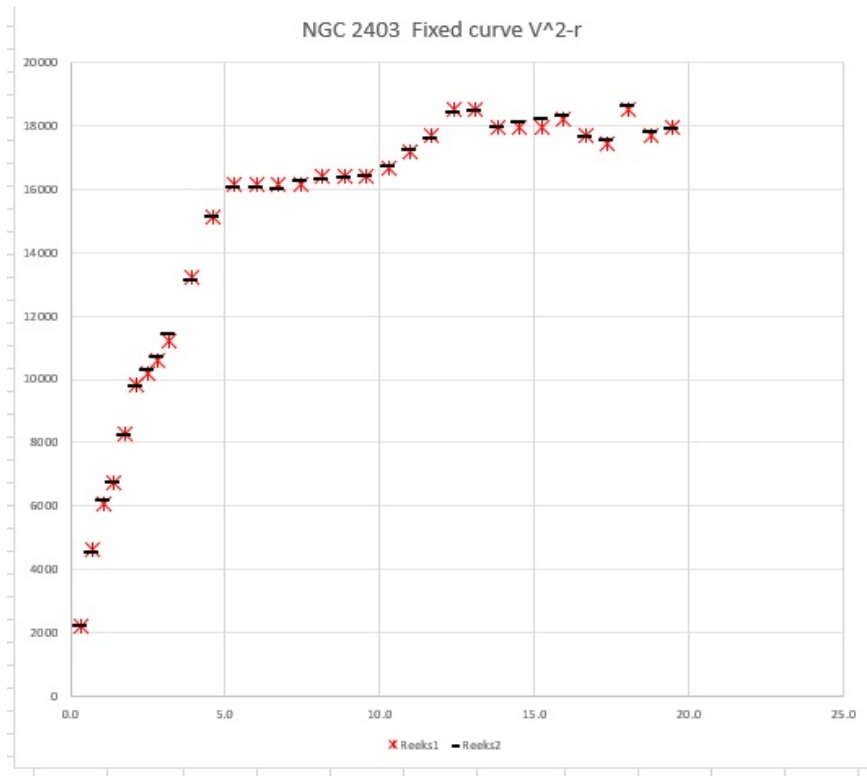


FIG. 5. UGC 2403 Plot1, V_{orb}^2 against r , fixed model.

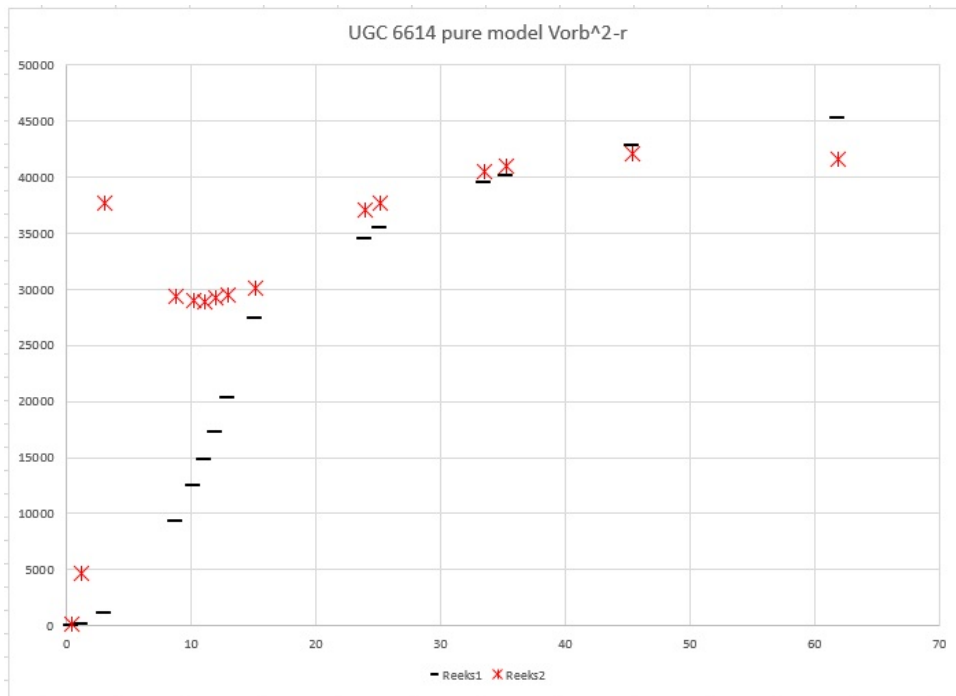


FIG. 6. UGC 6614 Plot1, V_{orb}^2 against r , pure model.

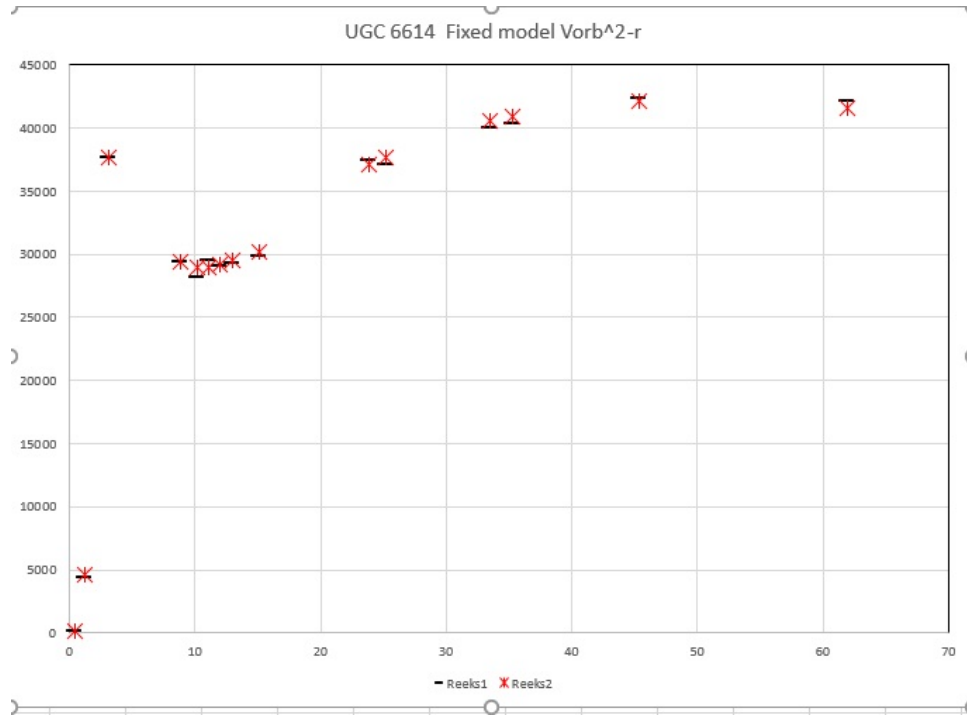


FIG. 7. UGC 6614 Plot1, V_{orb}^2 against r , fixed model.

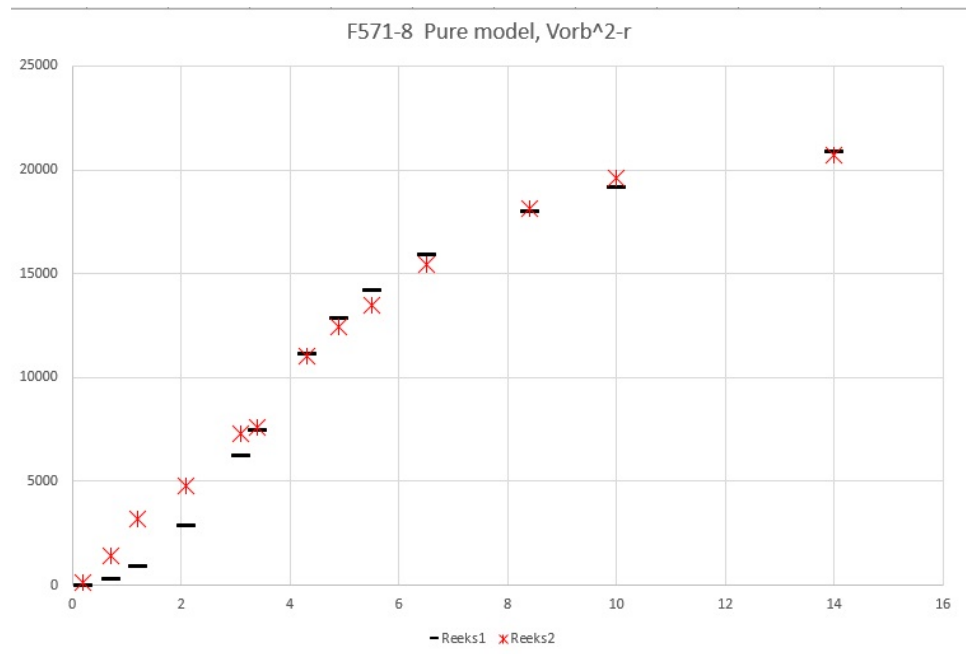


FIG. 8. F571-8 Plot1, V_{orb}^2 against r , pure model.

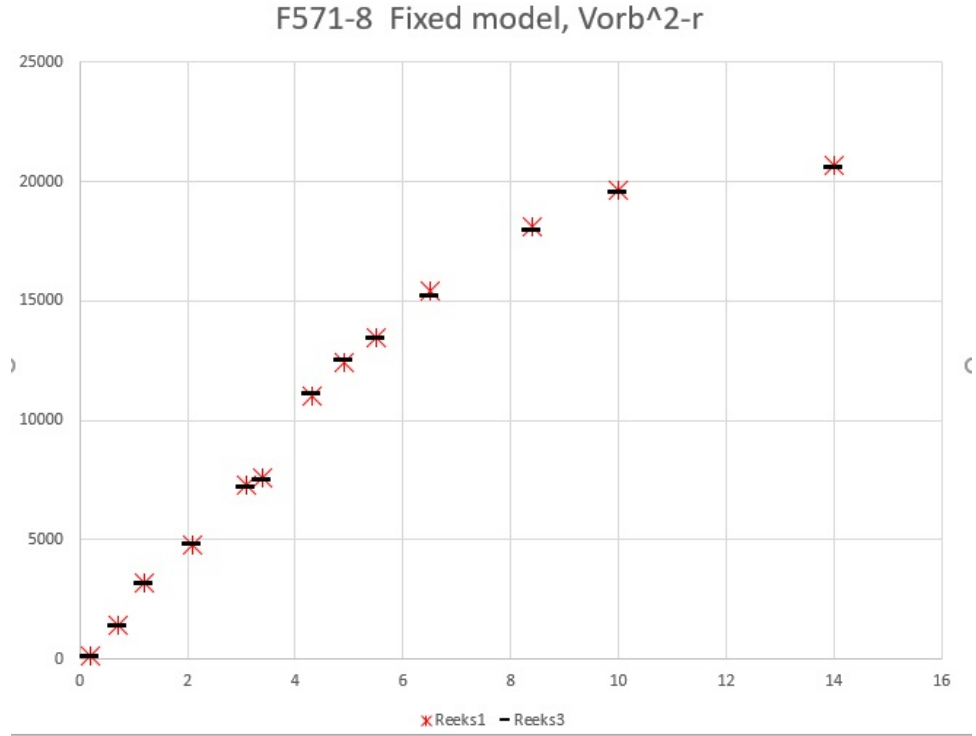


FIG. 9. F571-8 Plot1, V_{orb}^2 against r , fixed model.

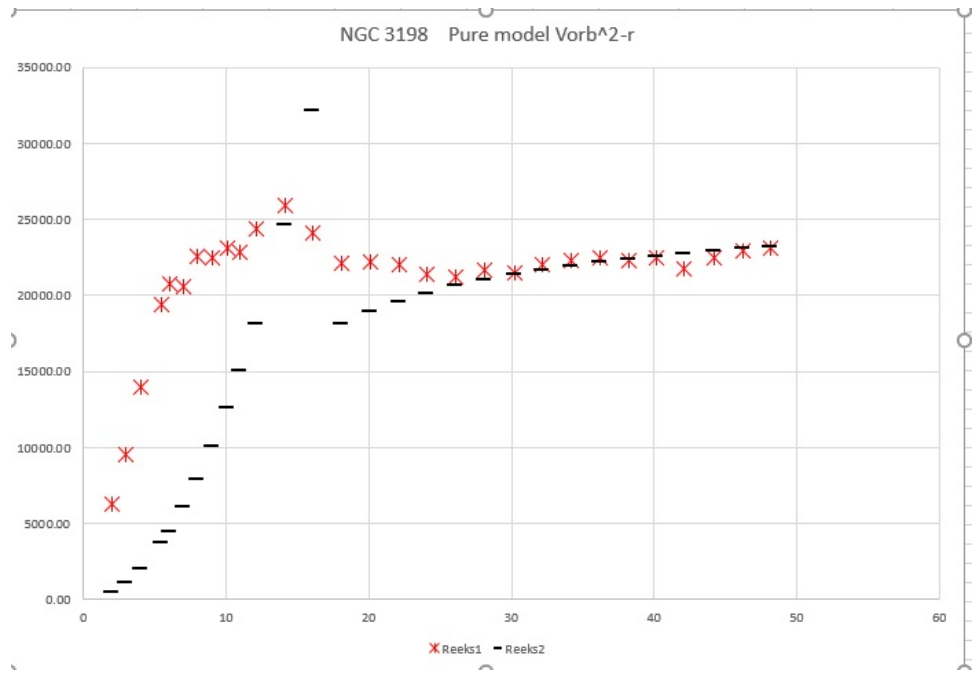


FIG. 10. NGC 3198 Plot1, V_{orb}^2 against r , pure model.

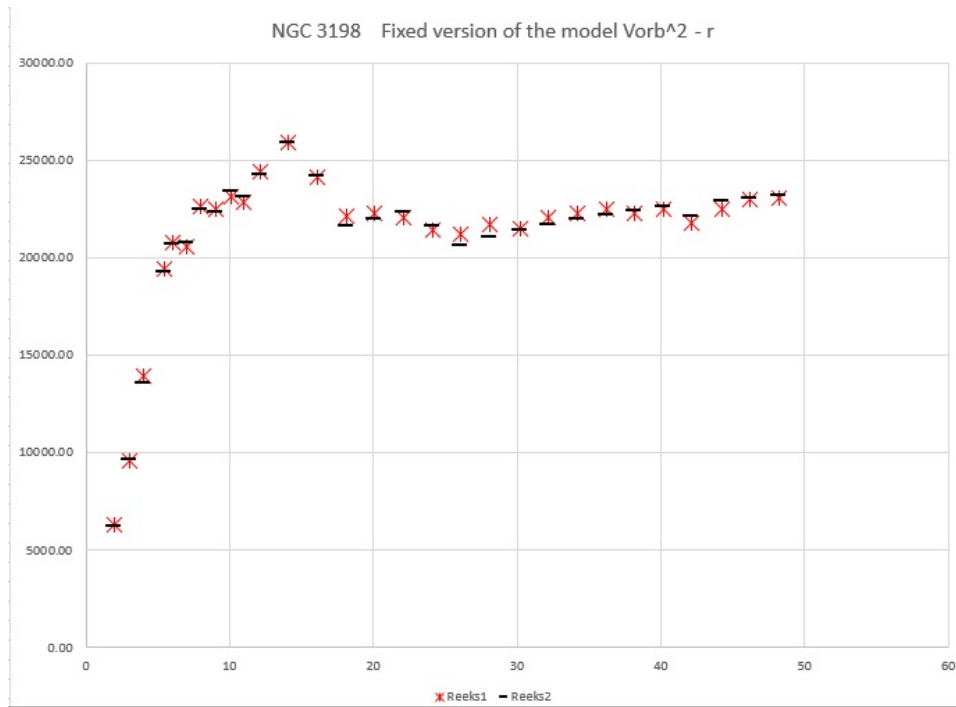


FIG. 11. NGC 3198 Plot1, V_{orb}^2 against r , fixed model.

VII. DARK MATTER, AN UNRESOLVED ISSUE

What about ‘dark matter’ and Dark Matter? Well, the early assumption of Oort and Zwicky that the astronomers were not seeing a lot of ordinary matter, the ‘dark matter’ postulate, turned out to be falsified. The attention then turned towards Dark Matter in the sense of non-baryonic (=non-ordinary Standard Model) stuff. The search for Dark Matter continues at ever increasing strengths.

My model galaxy, obeying to the ‘constant Lagrangian’ condition, just focuses on one aspect related to Dark Matter, the galactic rotation velocity curves. There are more issues leading to the Dark Matter hypothesis, unrelated to my model galaxy approach. Such as gravitational lensing, the galaxy cluster virial problem and cosmology related issues.

I have shown in four rotation fitting curves that my proposed model galaxies ‘constant Lagrangian’ postulate works in a limited number of situations. I also gave a theoretical context in which the ‘constant Lagrangian’ postulate might replace the classical virial theorem on a galactic scale. But it isn’t a ‘general law of nature’ because in the solar system and in the GNSS relativistic context, the classical virial theorem is proven accurate.

The question regarding Dark Matter depends on the status of the ‘constant Lagrangian’ postulate. If it is a cosmological law of nature, then we don’t need Dark Matter. But then we do need to explain why the classical virial theorem is valid in the context of the solar system. If Einstein’s theory is fundamental, then Newton’s needs to be justified. If the ‘constant Lagrangian’ postulate only functions (if it functions in that context in the first place) at the scale of individual galaxies, then the postulate needs further justification. A Dark Matter density distribution curve can easily provide such a justification.

The fact that it turned out to be possible to exactly plot the rotation curves with just one free parameter might indicate towards the underlying physics. In my approach, one free parameter can force a time-bubble on a whole galaxy. One free parameter needed to enforce a galactic time-bubble condition might well indicate a Dark Matter density distribution.

The problem with deriving a Dark Matter density distribution function from my postulate is that one then mixes two mutually exclusive axiomatic systems. I would have to add the classical energy situation, as expected according to the classical virial theorem, to my $L = K - V$ plot, drawn in a geodetic context where F_g is supposed to be zero. It can be done quite easily, but at the price of mixing mutually exclusive theoretical axiomatic approaches.

This mixing of axioms results for $r > R$ in

$$\rho_{DM} = \frac{3M}{4\pi} \left(\frac{2}{Rr} - \frac{2}{r^2} - \frac{1}{r^2} \ln \left(\frac{r}{R} \right) \right) \quad (23)$$

or, with $\rho_0 = M/V = 3M/4\pi R$, in

$$\rho_{DM} = \rho_0 \left(\frac{2R^2}{r} - \frac{2R^3}{r^2} - \frac{R^3}{r^2} \ln \left(\frac{r}{R} \right) \right), \quad (24)$$

with M and R referring to the mass and the radius of the pure model galactic bulge.

I can conclude that the ‘constant Lagrangian’ postulate leads to an interesting model galaxy and that the pure model can be adjusted using the two key parameters, the model bulge’s mass M and radius R , to match the four galaxy rotation curves to which is was exposed. Once the pure model parameters of M and R are chosen, only one of those parameters remains as a degree of freedom because the other one is then given through L . The model itself doesn’t decide on the existence of Dark Matter, because the postulate doesn’t justify itself but is in need of external justification. On that level will the Dark Matter discussion play out. The model is presented in the context of Special and General relativity, it is a metric approach with the Schwarzschild metric and the related time dilation formula at its core. As such, it might be an interesting addition to the MOND approach towards galactic and cosmological virial theorem issues.

REFERENCES

- Ashby, N. (2002, May). Relativity and the global positioning system. *Physics Today* 55(5), 41–47.
- Begeman, K. (2006). *HI rotation curves of spiral galaxies*. Ph. D. thesis. date submitted:2006
Rights: University of Groningen.
- Delva, P. and J. Lodewyck (2013). Atomic clocks: new prospects in metrology and geodesy.
In *Workshop on Relativistic Positioning Systems and their Scientific Applications Brdo, Slovenia, September 19-21, 2012*. arXiv:1308.6766 [physics.atom-ph].
- Hećimović, Ž. (2013). Relativistic effects on satellite navigation. *Tehnički vjesnik* 20(1), 195–203.
- Karukes, E. V., P. Salucci, and G. Gentile (2015). The dark matter distribution in the spiral NGC 3198 out to $0.22 R_{vir}$. *Astron. Astrophys.* 578, A13.
- Koopmans, L. et al. (2009). Strong gravitational lensing as a probe of gravity, dark-matter and super-massive black holes. *Astrophysical Journal*. [arXiv:astro-ph/0902.3186v2](https://arxiv.org/abs/0902.3186v2).
- McGaugh, S. S. (2005). The baryonic tully-fisher relation of galaxies with extended rotation curves and the stellar mass of rotating galaxies. *The Astrophysical Journal* 632, 859–871. [arXiv:astro-ph/0506750v2](https://arxiv.org/abs/astro-ph/0506750v2).
- McGaugh, S. S., V. C. Vera C. Rubin, and W. J. G. de Blok (2001). High-resolution rotation curves of low surface brightness galaxies. i. data. *The Astronomical Journal* 122(5), 2381.
- Mercier, C. (2015). Calculation of the apparent mass of the universe. [Website access](#) (accessed on April, 14, 2018).
- Milgrom, M. (1983a). A modification of the newtonian dynamics - implications for galaxies. *The Astrophysical Journal* 270, 371–387. [Astronomy Abstract Service pdf](#).
- Milgrom, M. (1983b). A modification of the newtonian dynamics as a possible alternative to the hidden mass hypothesis. *The Astrophysical Journal* 270, 365–370. [Astronomy Abstract Service](#).
- Misner, C., K. Thorne, and J. Wheeler (1973). *Gravitation*. San Francisco: Freeman and Company.
- Ohanian, H. and R. Ruffini (2013). *Gravitation and Spacetime* (3 ed.). New York: Cambridge University Press.
- Oort, J. H. (1932). The force exerted by the stellar system in the direction perpendicular

- to the galactic plane and some related problems. *Bulletin of the Astronomical Institutes of the Netherlands* 6, 249–287.
- Rubin, V., N. Thonnard, and W. J. Ford (1978). Extended rotation curves of high-luminosity spiral galaxies. iv - systematic dynamical properties, sa through sc. *Astrophysical Journal, Part 2 - Letters to the Editor* 225, L107–L111.
- Rubin, V., N. Thonnard, and W. J. Ford (1980). Rotational properties of 21 sc galaxies with a large range of luminosities and radii from ngc 4605 (r=4kpc) to ugc 2885 (r=122kpc). *Astrophysical Journal* 238, 471–487.
- Ruggiero, M. L., D. Bini, A. Gerialico, and A. Tartaglia (2008). Emission versus fermi coordinates: applications to relativistic positioning systems. *Classical and Quantum Gravity* 25(20), 205011. arXiv:0809.0998 [gr-qc].
- Singer, S. F. (1956). Application of an artificial satellite to the measurement of the general relativistic "red shift". *Phys. Rev.* 104, 11–14.
- Straumann, N. (1984). *General Relativity and Relativistic Astrophysics*. Berlin: Springer-Verlag.
- The ATLAS Collaboration (2018). Search for dark matter produced in association with bottom or top quarks in $\sqrt{s} = 13\text{tevpp}$ collisions with the atlas detector. *The European Physical Journal C* 78(1), 18.
- Tully, R. B. and J. R. Fisher (1977). A new method of determining distances to galaxies. *Astronomy and Astrophysics* 54, 661–673.
- Vossos, S. and E. Vossos (2017). Explanation of rotation curves in galaxies and clusters of them, by generalization of schwarzschild metric and combination with mond, eliminating dark matter. *Journal of Physics: Conference Series* 936(1), 012008.
- Weinberg, S. (1972). *Gravitation and cosmology: principles and applications of the general theory of relativity*. New York: Wiley & Sons.
- Zwicky, F. (1933). Die rotverschiebung von extragalaktischen nebeln. *Helvetica Physica Acta* 6, 110–127.
- Zwicky, F. (1937). On the masses of nebulae and of clusters of nebulae. *Astrophysical Journal* 86, 217–247.

15	R ² kpc ²	R arcsec	R kpc	V km/s	Vmodel	V (km/s) ²	V ² mode	unit GM/R	Mfix	Rfix	fix GM/R	$\frac{p_{\text{bulge}}}{p_{\text{total}}}$	3MG/R	Vfinal km/s
	0.13	22.5	0.4	47	10	2209	97	4.33E+04	0.48	3	6.92E+03	4.2	2.08E+04	144
	0.50	45	0.7	66	20	4624	386	43253	0.48	3	6.92E+03	4.2	2.08E+04	144
	1.13	67.5	1.1	78	29	6084	869	43253	0.48	3	6.92E+03	4.2	2.08E+04	144
	2.01	90	1.4	82	39	6724	1545	43253	0.48	3	6.92E+03	4.2	2.08E+04	144
	3.14	112.5	1.8	91	49	8281	2414	43253	0.48	3	6.92E+03	4.2	2.08E+04	144
	4.52	135	2.1	99	59	9801	3476	43253	0.48	3	6.92E+03	4.2	2.08E+04	144
	6.15	157.5	2.5	101	69	10201	4732	43253	0.48	3	6.92E+03	4.2	2.08E+04	144
	8.04	180	2.8	103	78	10609	6115	43253	0.48	3	6.92E+03	4.2	2.08E+04	144
	10.17	202.5	3.2	106	88	11236	7742	43253	0.48	3	6.92E+03	4.2	2.08E+04	144
	15.20	247.5	3.9	115	101	13225	10110	43253	0.48	3	6.92E+03	4.2	2.08E+04	144
	21.22	292.5	4.6	123	108	15129	11748	43253	0.48	3	6.92E+03	4.2	2.08E+04	144
	28.26	337.5	5.3	127	114	16129	12950	43253	0.48	3	6.92E+03	4.2	2.08E+04	144
	36.29	382.5	6.0	127	118	16129	13869	43253	0.48	3	6.92E+03	4.2	2.08E+04	144
	45.33	427.5	6.7	127	121	16129	14595	43253	0.48	3	6.92E+03	4.2	2.08E+04	144
	55.38	472.5	7.4	127	123	16129	15182	43253	0.48	3	6.92E+03	4.2	2.08E+04	144
	66.43	517.5	8.2	128	125	16384	15667	43253	0.48	3	6.92E+03	4.2	2.08E+04	144
	78.49	562.5	8.9	128	127	16384	16075	43253	0.48	3	6.92E+03	4.2	2.08E+04	144
	91.55	607.5	9.6	128	128	16384	16422	43253	0.48	3	6.92E+03	4.2	2.08E+04	144
	105.61	652.5	10.3	129	129	16641	16721	43253	0.48	3	6.92E+03	4.2	2.08E+04	144
	120.68	697.5	11.0	131	130	17161	16982	43253	0.48	3	6.92E+03	4.2	2.08E+04	144
	136.76	742.5	11.7	133	131	17689	17211	43253	0.48	3	6.92E+03	4.2	2.08E+04	144
	153.84	787.5	12.4	136	132	18496	17414	43253	0.48	3	6.92E+03	4.2	2.08E+04	144
	171.92	832.5	13.1	136	133	18496	17595	43253	0.48	3	6.92E+03	4.2	2.08E+04	144
	191.01	877.5	13.8	134	133	17956	17757	43253	0.48	3	6.92E+03	4.2	2.08E+04	144
	211.10	922.5	14.5	134	134	17956	17904	43253	0.48	3	6.92E+03	4.2	2.08E+04	144
	232.20	967.5	15.2	134	134	17956	18037	43253	0.48	3	6.92E+03	4.2	2.08E+04	144
	254.30	1012.5	15.9	135	135	18225	18158	43253	0.48	3	6.92E+03	4.2	2.08E+04	144
	277.41	1057.5	16.7	133	135	17689	18269	43253	0.48	3	6.92E+03	4.2	2.08E+04	144
	301.52	1102.5	17.4	132	136	17424	18370	43253	0.48	3	6.92E+03	4.2	2.08E+04	144
	326.64	1147.5	18.1	136	136	18496	18464	43253	0.48	3	6.92E+03	4.2	2.08E+04	144
	352.76	1192.5	18.8	133	136	17689	18551	43253	0.48	3	6.92E+03	4.2	2.08E+04	144
	379.88	1237.5	19.5	134	136	17956	18631	43253	0.48	3	6.92E+03	4.2	2.08E+04	144

FIG. 12. UGC 2403 Excell datasheet 1, V_{orb}^2 against r , pure model.

													pbulge=3M(4*3.14*R^3)*1000		
													pfixed		
R^2 kpc^2	R arosec	R kpc	V km/s	Vmodel	V (km/s)^2	V^2model	unit GMR	Mfix	Rfix	fix GMR	pbulge	3MG/R	Vfinal km/s		
0.13	22.5	0.4	47	47	2209	2225	4.33E+04	0.1	0.625	6.92E+03	97.8	2.08E+04	144		
0.50	45	0.7	68	67	4624	4541	43253	0.14	0.875	6.92E+03	49.9	2.08E+04	144		
1.13	67.5	1.1	78	79	6084	6180	43253	0.18	1.125	6.92E+03	30.2	2.08E+04	144		
2.01	90	1.4	82	82	6724	6729	43253	0.23	1.4375	6.92E+03	18.5	2.08E+04	144		
3.14	112.5	1.8	91	91	8281	8228	43253	0.26	1.625	6.92E+03	14.5	2.08E+04	144		
4.52	135	2.1	99	99	9801	9792	43253	0.286	1.7875	6.92E+03	12.0	2.08E+04	144		
6.15	157.5	2.5	101	101	10201	10300	43253	0.3	1.875	6.92E+03	10.9	2.08E+04	144		
8.04	180	2.8	103	103	10609	10692	43253	0.33	2.0625	6.92E+03	9.0	2.08E+04	144		
10.17	202.5	3.2	106	107	11236	11404	43253	0.345	2.1563	6.92E+03	8.2	2.08E+04	144		
15.20	247.5	3.9	115	114	13225	13105	43253	0.345	2.1563	6.92E+03	8.2	2.08E+04	144		
21.22	292.5	4.6	123	123	15129	15128	43253	0.3	1.875	6.92E+03	10.9	2.08E+04	144		
28.26	337.5	5.3	127	127	16129	16042	43253	0.29	1.8125	6.92E+03	11.6	2.08E+04	144		
36.29	382.5	6.0	127	127	16129	16023	43253	0.33	2.0625	6.92E+03	9.0	2.08E+04	144		
45.33	427.5	6.7	127	127	16129	16008	43253	0.37	2.3125	6.92E+03	7.1	2.08E+04	144		
55.38	472.5	7.4	127	127	16129	16228	43253	0.39	2.4375	6.92E+03	6.4	2.08E+04	144		
66.43	517.5	8.2	128	128	16384	16304	43253	0.42	2.625	6.92E+03	5.5	2.08E+04	144		
78.49	562.5	8.9	128	128	16384	16368	43253	0.45	2.8125	6.92E+03	4.8	2.08E+04	144		
91.55	607.5	9.6	128	128	16384	16422	43253	0.48	3	6.92E+03	4.2	2.08E+04	144		
105.61	652.5	10.3	129	129	16641	16721	43253	0.48	3	6.92E+03	4.2	2.08E+04	144		
120.68	697.5	11.0	131	131	17161	17218	43253	0.45	2.8125	6.92E+03	4.8	2.08E+04	144		
136.76	742.5	11.7	133	133	17689	17581	43253	0.43	2.6875	6.92E+03	5.3	2.08E+04	144		
153.84	787.5	12.4	136	136	18496	18390	43253	0.34	2.125	6.92E+03	8.5	2.08E+04	144		
171.92	832.5	13.1	136	136	18496	18452	43253	0.35	2.1875	6.92E+03	8.0	2.08E+04	144		
191.01	877.5	13.8	134	134	17956	17945	43253	0.45	2.8125	6.92E+03	4.8	2.08E+04	144		
211.10	922.5	14.5	134	134	17956	18082	43253	0.45	2.8125	6.92E+03	4.8	2.08E+04	144		
232.20	967.5	15.2	134	135	17956	18207	43253	0.45	2.8125	6.92E+03	4.8	2.08E+04	144		
254.30	1012.5	15.9	135	135	18225	18321	43253	0.45	2.8125	6.92E+03	4.8	2.08E+04	144		
277.41	1057.5	16.7	133	133	17689	17645	43253	0.6	3.75	6.92E+03	2.7	2.08E+04	144		
301.52	1102.5	17.4	132	132	17424	17523	43253	0.65	4.0625	6.92E+03	2.3	2.08E+04	144		
326.64	1147.5	18.1	136	136	18496	18608	43253	0.45	2.8125	6.92E+03	4.8	2.08E+04	144		
352.76	1192.5	18.8	133	133	17689	17768	43253	0.65	4.0625	6.92E+03	2.3	2.08E+04	144		
379.88	1237.5	19.5	134	134	17956	17877	43253	0.65	4.0625	6.92E+03	2.3	2.08E+04	144		

FIG. 13. UGC 2403 Excell datasheet 1, V_{orb}^2 against r , fixed model.

Rkpc	R^2	fix GM/R	V^2 mode	Vexp^2	Vmodel	Vexp	Vdisk^2	Vbulge^2	unit GM/R	Mfix	Rfix	fix GM/R	pbulge	3MG/R	Vfinal km/s
0.4	0.16	1.73E+04	19	172	4.4	13.1	98	484	4.33E+04	4.8	12	1.73E+04	0.7	5.19E+04	228
1.2	1.44	1.73E+04	173	4651	13.2	68.2	767	3831.61	43253	4.8	12	1.73E+04	0.7	5.19E+04	228
3.1	9.61	1.73E+04	1155	37636	34.0	194	1706	9781.21	43253	4.8	12	1.73E+04	0.7	5.19E+04	228
8.8	77.44	1.73E+04	9304	29412	96.5	171.5	1962	5461.21	43253	4.8	12	1.73E+04	0.7	5.19E+04	228
10.2	104.04	1.73E+04	12500	28968	111.8	170.2	2088	4774.81	43253	4.8	12	1.73E+04	0.7	5.19E+04	228
11.1	123.21	1.73E+04	14803	28934	121.7	170.1	2314	4395.69	43253	4.8	12	1.73E+04	0.7	5.19E+04	228
12	144	1.73E+04	17301	29207	132	170.9	2611	4096	43253	4.8	12	1.73E+04	0.7	5.19E+04	228
13	169	1.73E+04	20305	29515	142	171.8	3025	3782.25	43253	4.8	12	1.73E+04	0.7	5.19E+04	228
15.1	228.01	1.73E+04	27395	30137	166	173.6	3745	3249	43253	4.8	12	1.73E+04	0.7	5.19E+04	228
23.9	571.21	1.73E+04	34530	37095	186	192.6	3552	2052.09	43253	4.8	12	1.73E+04	0.7	5.19E+04	228
25.2	635.04	1.73E+04	35427	37675	188	194.1	3329	1953.64	43253	4.8	12	1.73E+04	0.7	5.19E+04	228
33.5	1122.25	1.73E+04	39509	40522	199	201.3	2970	1459.24	43253	4.8	12	1.73E+04	0.7	5.19E+04	228
35.3	1246.09	1.73E+04	40141	40925	200	202.3	3170	1383.84	43253	4.8	12	1.73E+04	0.7	5.19E+04	228
45.4	2061.16	1.73E+04	42758	42107	207	205.2	2884	1082.41	43253	4.8	12	1.73E+04	0.7	5.19E+04	228
61.9	3831.61	1.73E+04	45196	41575	213	203.9	1858	795.24	43253.4	4.8	12	1.73E+04	0.7	5.19E+04	228

FIG. 14. UGC 6614 Excell datasheet 1, V_{orb}^2 against r , pure model.

Rkpc	R^2	GM/R	V^2 model	Vexp^2	Vmodel	Vexp	Vdisk^2	Vbulge^2	unit GM/R Mfix	Rfix	fix GM/R	pbulge	3MG/R	Vfinal km/s	
0.4	0.16	1.73E+04	197	172	14.0	13.1	98	484	4.33E+04	1.5	3.75	1.73E+04	6.8	5.19E+04	228
1.2	1.44	1.73E+04	4417	4651	66.5	68.2	767	3831.61	43253	0.95	2.38	1.73E+04	16.9	5.19E+04	228
3.1	9.61	1.73E+04	37702	37636	194.2	194	1706	9781.21	43253	0.84	2.10	1.73E+04	21.7	5.19E+04	228
8.8	77.44	1.73E+04	29406	29412	171.5	171.5	1962	5461.21	43253	2.7	6.75	1.73E+04	2.1	5.19E+04	228
10.2	104.04	1.73E+04	28126	28968	167.7	170.2	2088	4774.81	43253	3.2	8.00	1.73E+04	1.5	5.19E+04	228
11.1	123.21	1.73E+04	29505	28934	171.8	170.1	2314	4395.69	43253	3.4	8.50	1.73E+04	1.3	5.19E+04	228
12	144	1.73E+04	29118	29207	171	170.9	2611	4096	43253	3.7	9.25	1.73E+04	1.1	5.19E+04	228
13	169	1.73E+04	29239	29515	171	171.8	3025	3782.25	43253	4	10.00	1.73E+04	1.0	5.19E+04	228
15.1	228.01	1.73E+04	29829	30137	173	173.6	3745	3249	43253	4.6	11.50	1.73E+04	0.7	5.19E+04	228
23.9	571.21	1.73E+04	37426	37095	193	192.6	3552	2052.09	43253	4	10.00	1.73E+04	1.0	5.19E+04	228
25.2	635.04	1.73E+04	37143	37675	193	194.1	3329	1953.64	43253	4.3	10.75	1.73E+04	0.8	5.19E+04	228
33.5	1122.25	1.73E+04	40026	40522	200	201.3	2970	1459.24	43253	4.6	11.50	1.73E+04	0.7	5.19E+04	228
35.3	1246.09	1.73E+04	40386	40925	201	202.3	3170	1383.84	43253	4.7	11.75	1.73E+04	0.7	5.19E+04	228
45.4	2061.16	1.73E+04	42377	42107	206	205.2	2884	1082.41	43253	5	12.50	1.73E+04	0.6	5.19E+04	228
61.9	3831.61	1.73E+04	42121	41575	205	203.9	1858	795.24	43253.4	7	17.50	1.73E+04	0.3	5.19E+04	228

FIG. 15. UGC 6614 Excell datasheet 1, V_{orb}^2 against r , fixed model.

fix		G =	6.674E-11	GMunit/Runit =	4.33E+10 (m/s)^2 = Vunit^2										
		Runit=	1kpc = 3.086E+19 meter	Vunit =	208 km/s										
		Munit=	1E+10*Mo = 2.00E+40 kg	Vunit^2 =	43227 (km/s)^2										
		$\rho_{bulge}=3M/(4*\pi*R^3)*1000$													
Rkpc	GM/R	V^2 mode	V^2	Vmodel	Vexp	Vdisk^2	Vbulge^2	unit GM/R Mfix	Rfix	fix GM/R	pbulge	3MG/R	Vfinal km/s		
0.2	8.41E+03	26	154	5.1	12.4	31	289	4.33E+04	0.7	3.6	8.41E+03	3.6	2.52E+04	159	
0.7	8.41E+03	318	1406	17.8	37.5	250	2052	43253	0.7	3.6	8.41E+03	3.6	2.52E+04	159	
1.2	8.41E+03	934	3192	30.6	56.5	548	3376	43253	0.7	3.6	8.41E+03	3.6	2.52E+04	159	
2.1	8.41E+03	2862	4775	53.5	69.1	1056	2959	43253	0.7	3.6	8.41E+03	3.6	2.52E+04	159	
3.1	8.41E+03	6236	7310	79.0	85.5	1505	2228	43253	0.7	3.6	8.41E+03	3.6	2.52E+04	159	
3.4	8.41E+03	7502	7586	86.6	87.1	1576	2061	43253	0.7	3.6	8.41E+03	3.6	2.52E+04	159	
4.3	8.41E+03	11149	11025	106	105	1798	1560	43253	0.7	3.6	8.41E+03	3.6	2.52E+04	159	
4.9	8.41E+03	12873	12455	113	111.6	1866	1362	43253	0.7	3.6	8.41E+03	3.6	2.52E+04	159	
5.5	8.41E+03	14221	13456	119	116	1910	1176	43253	0.7	3.6	8.41E+03	3.6	2.52E+04	159	
6.5	8.41E+03	15915	15426	126	124.2	1910	986	43253	0.7	3.6	8.41E+03	3.6	2.52E+04	159	
8.4	8.41E+03	18022	18117	134	134.6	1781	745	43253	0.7	3.6	8.41E+03	3.6	2.52E+04	159	
10	8.41E+03	19176	19628	138	140.1	1616	625	43253	0.7	3.6	8.41E+03	3.6	2.52E+04	159	
14	8.41E+03	20906	20707	145	143.9	1190	441	43253	0.7	3.6	8.41E+03	3.6	2.52E+04	159	

FIG. 16. F571 8 Excell datasheet 1, V_{orb}^2 against r , pure model.

fix		G =	6.674E-11	GMunit/Runit =	4.33E+10 (m/s)^2 = Vunit^2										
		Runit=	1kpc = 3.086E+19 meter	Vunit =	208 km/s										
		Munit=	1E+10*Mo = 2.00E+40 kg	Vunit^2 =	43227 (km/s)^2										
		$\rho_{bulge}=3M/(4*\pi*R^3)*1000$													
GM/R	Rkpc	V^2 model	V^2	Vmodel	Vexp	Vdisk^2	2Vbulge^2	unit GM/R Mfix	Rfix	fix GM/R	pbulge	3MG/R	Vfinal km/s		
8.41E+03	0.2	141	154	11.9	12.4	31		4.33E+04	0.3	1.5	8.41E+03	19.5	2.52E+04	159	
8.41E+03	0.7	1431	1406	37.8	37.5	250		43253	0.33	1.7	8.41E+03	16.1	2.52E+04	159	
8.41E+03	1.2	3171	3192	56.3	56.5	548	6751.22	43253	0.38	2.0	8.41E+03	12.2	2.52E+04	159	
8.41E+03	2.1	4809	4775	69.3	69.1	1056	5918.72	43253	0.54	2.8	8.41E+03	6.0	2.52E+04	159	
8.41E+03	3.1	7233	7310	85.0	85.5	1505	4455.68	43253	0.65	3.3	8.41E+03	4.2	2.52E+04	159	
8.41E+03	3.4	7502	7586	86.6	87.1	1576	4122.32	43253	0.7	3.6	8.41E+03	3.6	2.52E+04	159	
8.41E+03	4.3	11149	11025	106	105	1798	3120.5	43253	0.7	3.6	8.41E+03	3.6	2.52E+04	159	
8.41E+03	4.9	12520	12455	112	111.6	1866	2723.22	43253	0.72	3.7	8.41E+03	3.4	2.52E+04	159	
8.41E+03	5.5	13435	13456	116	116	1910	2352.98	43253	0.75	3.9	8.41E+03	3.1	2.52E+04	159	
8.41E+03	6.5	15250	15426	123	124.2	1910	1971.92	43253	0.75	3.9	8.41E+03	3.1	2.52E+04	159	
8.41E+03	8.4	18022	18117	134	134.6	1781	1490.58	43253	0.7	3.6	8.41E+03	3.6	2.52E+04	159	
8.41E+03	10	19608	19628	140	140.1	1616	1250	43253	0.65	3.3	8.41E+03	4.2	2.52E+04	159	
8.41E+03	14	20597	20707	144	143.9	1190	882	43253	0.75	3.9	8.41E+03	3.1	2.52E+04	159	

FIG. 17. F571 8 Excell datasheet 1, V_{orb}^2 against r , fixed model.

R ² kpc ²	R kpc	V km/s	Vmodel	V (km/s) ²	V ² model	unit GMR	Mfix	Rfix	fix GMR	pbulge	3MG/R	Vfinal km/s
4.00	2	79.00	22	6241.00	496	4.33E+04	1.7	8.4	8.75E+03	0.69	2.63E+04	162
9.00	3	97.80	33	9564.84	1117	43253	1.7	8.4	8.75E+03	0.69	2.63E+04	162
16.00	4	118.00	45	13924	1985	43253	1.7	8.4	8.75E+03	0.69	2.63E+04	162
30.25	5.5	139.40	61	19432.4	3753	43253	1.7	8.4	8.75E+03	0.69	2.63E+04	162
36.00	6	144.20	67	20793.6	4466	43253	1.7	8.4	8.75E+03	0.69	2.63E+04	162
49.00	7	143.30	78	20534.9	6079	43253	1.7	8.4	8.75E+03	0.69	2.63E+04	162
64.00	8	150.30	89	22590.1	7940	43253	1.7	8.4	8.75E+03	0.69	2.63E+04	162
81.00	9	149.90	100	22470	10049	43253	1.7	8.4	8.75E+03	0.69	2.63E+04	162
102.01	10.1	152.10	112	23134.4	12655	43253	1.7	8.4	8.75E+03	0.69	2.63E+04	162
121.00	11	151.10	123	22831.2	15011	43253	1.7	8.4	8.75E+03	0.69	2.63E+04	162
146.41	12.1	156.20	135	24398.4	18164	43253	1.7	8.4	8.75E+03	0.69	2.63E+04	162
198.81	14.1	161.00	157	25921	24664	43253	1.7	8.4	8.75E+03	0.69	2.63E+04	162
259.21	16.1	155.30	179	24118.1	32158	43253	1.7	8.4	8.75E+03	0.69	2.63E+04	162
327.61	18.1	148.70	135	22111.7	18136	43253	1.7	8.4	8.75E+03	0.69	2.63E+04	162
404.01	20.1	149.10	138	22230.8	18944	43253	1.7	8.4	8.75E+03	0.69	2.63E+04	162
488.41	22.1	148.40	140	22022.6	19607	43253	1.7	8.4	8.75E+03	0.69	2.63E+04	162
580.81	24.1	146.20	142	21374.4	20159	43253	1.7	8.4	8.75E+03	0.69	2.63E+04	162
681.21	26.1	145.50	144	21170.3	20626	43253	1.7	8.4	8.75E+03	0.69	2.63E+04	162
789.61	28.1	147.30	145	21697.3	21027	43253	1.7	8.4	8.75E+03	0.69	2.63E+04	162
912.04	30.2	146.50	146	21462.3	21391	43253	1.7	8.4	8.75E+03	0.69	2.63E+04	162
1036.84	32.2	148.40	147	22022.6	21694	43253	1.7	8.4	8.75E+03	0.69	2.63E+04	162
1169.64	34.2	149.30	148	22290.5	21961	43253	1.7	8.4	8.75E+03	0.69	2.63E+04	162
1310.44	36.2	149.90	149	22470	22199	43253	1.7	8.4	8.75E+03	0.69	2.63E+04	162
1459.24	38.2	149.30	150	22290.5	22411	43253	1.7	8.4	8.75E+03	0.69	2.63E+04	162
1616.04	40.2	150.00	150	22500	22603	43253	1.7	8.4	8.75E+03	0.69	2.63E+04	162
1772.41	42.1	147.60	151	21785.8	22768	43253	1.7	8.4	8.75E+03	0.69	2.63E+04	162
1953.64	44.2	149.80	151	22440	22934	43253	1.7	8.4	8.75E+03	0.69	2.63E+04	162
2134.44	46.2	151.50	152	22952.3	23078	43253	1.7	8.4	8.75E+03	0.69	2.63E+04	162
2323.24	48.2	151.90	152	23073.6	23210	43253	1.7	8.4	8.75E+03	0.69	2.63E+04	162

FIG. 18. NGC 3198 Excell datasheet 1, V_{orb}^2 against r , pure model.

R ² kpc ²	R kpc	V km/s	Vmodel	V (km/s) ²	V ² model	unit GMR	Mfix	Rfix	fix GMR	pbulge	3MG/R	Vfinal km/s
4.00	2	79.00	79	6241.00	6225	4.33E+04	0.48	2.4	8.75E+03	8.59	2.63E+04	162
9.00	3	97.80	98	9564.84	9592	43253	0.58	2.9	8.75E+03	5.89	2.63E+04	162
16.00	4	118.00	117	13924	13578	43253	0.65	3.2	8.75E+03	4.69	2.63E+04	162
30.25	5.5	139.40	139	19432.36	19281	43253	0.75	3.7	8.75E+03	3.52	2.63E+04	162
36.00	6	144.20	144	20793.6	20681	43253	0.79	3.9	8.75E+03	3.17	2.63E+04	162
49.00	7	143.30	144	20534.89	20756	43253	0.92	4.5	8.75E+03	2.34	2.63E+04	162
64.00	8	150.30	150	22590.09	22494	43253	1.01	5.0	8.75E+03	1.94	2.63E+04	162
81.00	9	149.90	149	22470.01	22346	43253	1.14	5.6	8.75E+03	1.52	2.63E+04	162
102.01	10.1	152.10	153	23134.41	23407	43253	1.25	6.2	8.75E+03	1.27	2.63E+04	162
121.00	11	151.10	152	22831.21	23114	43253	1.37	6.8	8.75E+03	1.05	2.63E+04	162
146.41	12.1	156.20	156	24398.44	24292	43253	1.47	7.3	8.75E+03	0.92	2.63E+04	162
198.81	14.1	161.00	161	25921	25867	43253	1.66	8.2	8.75E+03	0.72	2.63E+04	162
259.21	16.1	155.30	156	24118.09	24192	43253	1.96	9.7	8.75E+03	0.52	2.63E+04	162
327.61	18.1	148.70	147	22111.69	21625	43253	0.97	4.8	8.75E+03	2.10	2.63E+04	162
404.01	20.1	149.10	148	22230.81	21957	43253	1	4.9	8.75E+03	1.98	2.63E+04	162
488.41	22.1	148.40	149	22022.56	22347	43253	1	4.9	8.75E+03	1.98	2.63E+04	162
580.81	24.1	146.20	147	21374.44	21595	43253	1.3	6.4	8.75E+03	1.17	2.63E+04	162
681.21	26.1	145.50	144	21170.25	20626	43253	1.7	8.4	8.75E+03	0.69	2.63E+04	162
789.61	28.1	147.30	145	21697.29	21027	43253	1.7	8.4	8.75E+03	0.69	2.63E+04	162
912.04	30.2	146.50	146	21462.25	21391	43253	1.7	8.4	8.75E+03	0.69	2.63E+04	162
1036.84	32.2	148.40	147	22022.56	21694	43253	1.7	8.4	8.75E+03	0.69	2.63E+04	162
1169.64	34.2	149.30	148	22290.49	21961	43253	1.7	8.4	8.75E+03	0.69	2.63E+04	162
1310.44	36.2	149.90	149	22470.01	22199	43253	1.7	8.4	8.75E+03	0.69	2.63E+04	162
1459.24	38.2	149.30	150	22290.49	22411	43253	1.7	8.4	8.75E+03	0.69	2.63E+04	162
1616.04	40.2	150.00	150	22500	22603	43253	1.7	8.4	8.75E+03	0.69	2.63E+04	162
1772.41	42.1	147.60	149	21785.76	22151	43253	2	9.9	8.75E+03	0.49	2.63E+04	162
1953.64	44.2	149.80	151	22440.04	22934	43253	1.7	8.4	8.75E+03	0.69	2.63E+04	162
2134.44	46.2	151.50	152	22952.25	23078	43253	1.7	8.4	8.75E+03	0.69	2.63E+04	162
2323.24	48.2	151.90	152	23073.61	23210	43253	1.7	8.4	8.75E+03	0.69	2.63E+04	162

FIG. 19. NGC 3198 Excell datasheet 1, V_{orb}^2 against r , fixed model.